

Transforming Spatial Entanglement Using a Domain-Engineering Technique

X. Q. Yu,^{1,2} P. Xu,¹ Z. D. Xie,¹ J. F. Wang,¹ H. Y. Leng,¹ J. S. Zhao,¹ S. N. Zhu,^{1,*} and N. B. Ming¹

¹National Laboratory of Solid State Microstructures and Department of Physics, Nanjing University, Nanjing, 210093, China

²Physics Department, Southeast University, Nanjing, 211189, China

(Received 30 May 2008; published 1 December 2008)

We study the spatial correlation of a two-photon entangled state produced in a multistripe periodically poled LiTaO₃ crystal by spontaneous parametric down-conversion. The far-field diffraction-interference experiments reveal that the transverse modulation of domain patterns transforms the spatial mode function of the two-photon state. This result offers an approach to prepare a novel type of two-photon state with a unique spatial entanglement by using a domain-engineering technique.

DOI: 10.1103/PhysRevLett.101.233601

PACS numbers: 42.50.Dv, 42.50.Ct, 42.65.Lm, 77.80.Dj

The two-photon state, which is produced by spontaneous parametric down-conversion (SPDC), exhibits spatial entanglement in a finite- or infinite-dimensional Hilbert space [1–5]. Mathematically, such a spatial entanglement is embedded in the mode function of a two-photon state and plays an important role in the study of foundational quantum mechanics [6] and quantum communication [7,8]. Many nonclassical behaviors of the two-photon pair, such as quantum interference and quantum imaging, also rely heavily on the spatial structure of the mode function. Therefore an important issue in quantum optics is how to control the mode function of a two-photon pair or, in other words, how to prepare two-photon pairs with required spatial entanglement. As reported previously, in some cases, such a goal has been achieved by manipulating the beam profile of the pump laser [9,10] or by placing the spatial light modulators in the arms of the two-photon pair [11]. Recently, another scheme was put forward by Torres *et al.* in theory [12]. This scheme allows the two-photon spatial mode to be tailored and manipulated by transversely patterned quasi-phase-matched (QPM) gratings. But the issue is still open due to a lack of related studies, in particular, on the experiment aspect.

It is known that, in a QPM device, the modulated nonlinearity would affect the time-frequency and space-momentum properties of the generated two-photon pairs [13–19]. Especially, transverse modulation of nonlinearity can greatly influence the spatial properties of the down-converted beam. Fejer *et al.* and Qin *et al.* extended Huygens-Fresnel principle (HFP) from linear optics to parametric processes induced by quadratic nonlinearity [20,21]. It can be described that each point on the primary wave front acts as a source of secondary wavelets of the pump, as well as a source of the signal and idler waves in a parametric process. In this case the HFP can be used to engineer domain patterns in crystal for the aims of parametric beam focusing, shaping, or multifunction integration. In this Letter, we study the entangled state generated from a multistripe periodically poled LiTaO₃ (MPPLT) crystal, in which the longitudinal modulation of nonlinearity

works for QPM-SPDC, whereas the transverse modulation is used to manipulate the two-photon spatial mode. In our case, the pump, signal, and idler photons are all *e*-polarized, so the maximum quadratic nonlinearity component d_{33} is used. The work actually links up the HFP with a particular domain pattern to create and at the same time transform the spatial entanglement of photon pairs. The experimental results prove that the structure information of domain patterns is transferred into the spatial mode of an entangled state. By using this technique, it should also be convenient to control the effective finite Hilbert space related to the freedom of the transverse degree, such as the orbital angular momentum, and increase the efficiency of the quantum communications [22].

The MPPLT sample is sketched in Fig. 1(a), in which *N* stripes are periodically poled for collinear SPDC and arranged in parallel. When the pump beam waist is large enough, at a certain time, the two-photon pair can be produced from any one of the illuminated stripes, which

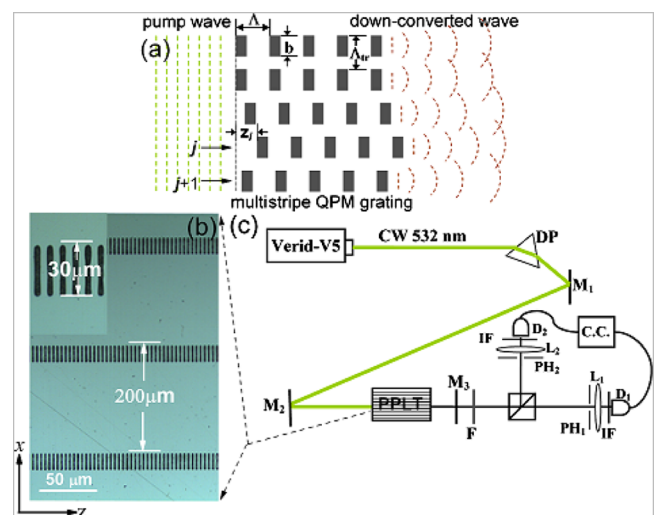


FIG. 1 (color online). (a) Schematic diagram of the nonlinear HFP principle and the multistripe QPM structure. (b) Micrograph of the MPPLT. (c) Experimental setup.

can be regarded as a coherent SPDC subsource. The generated two-photon state is a superposition of all of the possible states: $|\Psi\rangle = \sum_{j=1}^N c_j e^{i\phi_j} |j, j\rangle$, where $|j, j\rangle$ corresponds to a photon pair created from the j th stripe and c_j is the relative amplitude and is proportional to the j th stripe volume V_j and the intensity of the pump beam. $\phi_j = 2\pi z_j/\Lambda$ is the relative phase, where z_j is the initial coordinate of the j th stripe along the z axis and Λ the longitudinal modulation period of domain. By adjusting the volume and initial position of each stripe, in principle, we could get any spatial mode of down-converted photon pairs according to the HFP as shown in Fig. 1(a). In the following parts, we will derive the mode function of this case.

In the interaction picture, the effective Hamiltonian for SPDC is given by

$$H_1 = \varepsilon_0 \int_V d^3r \chi^{(2)} E_p^{(+)} E_s^{(-)} E_i^{(-)} + \text{H.c.}, \quad (1)$$

where H.c. stands for the Hermitian conjugate and V is the interaction volume. $\chi^{(2)}$ is the quadratic nonlinear susceptibility of the crystal. The positive frequency part of the quantized field is $E_j^{(+)} = \sum_{\vec{k}_j} E_j e^{i(\vec{k}_j \cdot \vec{r} - \omega_j t)} a_j(\vec{k}_j)$, where $\vec{\omega}_j$, \vec{k}_j ($j = s, i, p$) are the angular frequencies and the wave vectors of signal, idler, and pump, respectively, $a_{s(i)}$ is the annihilation operator of signal (idler) photon, $E_j = i\sqrt{\hbar\omega_j/(2\varepsilon_0 n_j^2 V_Q)}$, and V_Q is the quantization volume. For simplicity, we assume the pump field to be nondepleted, monochromatic, and classical.

The longitudinal and transverse modulation of $\chi^{(2)}$ in the MPPLT is separable under our experimental condition. We can show that

$$\chi^{(2)}(\vec{r}) = U(\vec{\rho}) \sum_m f(G_m) e^{-iG_m z}, \quad (2)$$

where the subscript m refers to the m th component of the Fourier series with coefficient $f(G_m)$ and the reciprocal vector $G_m = 2m\pi/\Lambda$ and $U(\vec{\rho})$ is the transverse modulation function of the multistriple grating. Generally, the first-order reciprocal vector G_1 is designed to satisfy the longitudinal phase-matching condition. Under the first-order perturbation approximation, the two-photon state is

$$|\Psi\rangle = g \sum_{\vec{k}_s, \vec{k}_i} \Phi(\Delta k_z L) H_{\text{tr}}(\vec{k}_s + \vec{k}_i) \times \delta(\omega_p - \omega_s - \omega_i) \hat{a}_s^\dagger \hat{a}_i^\dagger |0\rangle, \quad (3)$$

where

$$H_{\text{tr}}(\vec{k}_s + \vec{k}_i) = (1/A) \int_A d^2\rho E_p(\vec{\rho}) U(\vec{\rho}) e^{-i(\vec{k}_s + \vec{k}_i) \cdot \vec{\rho}} = \mathcal{F}\{E_p(\vec{\rho}) U(\vec{\rho})\}. \quad (4)$$

We have assumed that the beam size A is large enough. The longitudinal mode function $\Phi(\Delta k_z L) = \sin(\Delta k_z L)/(\Delta k_z L)$, where $\Delta k_z = k_p - k_{sz} - k_{iz} - G_1$ is the phase mismatching in longitudinal z direction, L the stripe length, and $\kappa_{s(i)}$ the transverse wave vector of the signal (idler) photon. It is noteworthy that the transverse mode function H_{tr} is the Fourier transform of the function $E_p \cdot U$, so the transverse information of the MPPLT is transferred to the spatial mode of the generated two-photon state. In our case, there is no modulation in the y axis, so we just consider the modulation along the x axis, and then H_{tr} is expressed by

$$H_x(k_{s,x} + k_{i,x}) \propto \frac{\sin[N(k_{s,x} + k_{i,x})\Lambda_{\text{tr}}/2]}{\sin[(k_{s,x} + k_{i,x})\Lambda_{\text{tr}}/2]} \times \text{sinc}[(k_{s,x} + k_{i,x})b/2]. \quad (5)$$

In Eq. (5), Λ_{tr} and b represent the stripe interval and the strip width, respectively. This is a standard far-field diffraction-interference pattern of a multislit. Thus the coincidence counting rate in the far-field region can be derived:

$$R_c(x_1, x_2) = \langle \Psi | E_1^{(-)} E_2^{(-)} E_2^{(+)} E_1^{(+)} | \Psi \rangle \propto \left| H_x \left(\frac{\omega_s x_1}{c z_1} + \frac{\omega_i x_2}{c z_2} \right) \right|^2, \quad (6)$$

where E_1 (E_2) is the field operator at detector D_1 (D_2), c the velocity of light in vacuum, x_1 (x_2) the horizontal position of detector D_1 (D_2) in the detecting plane, and z_1 (z_2) the distance between the output face of the crystal and the detecting plane.

The theoretical result above was proved by the coincidence measurement on the two-photon pairs in the far-field region. Figure 1(b) is the micrograph of the domain pattern of the etched MPPLT sample, showing the stripe interval $\Lambda_{\text{tr}} = 200 \mu\text{m}$ and stripe width $b = 30 \mu\text{m}$. The whole stripe length $L = 6 \text{ mm}$, and the effective stripe number $N = 4$ for the pumping beam waist of 1 mm. All stripes had the same longitudinal modulation period $\Lambda = 7.548 \mu\text{m}$. The sample was operated at 174.6 °C, which was the phase-matching temperature for the SPDC process. The degenerate 1064 nm photon pairs were generated collinearly as the sample was illuminated by a cw-532 nm laser. Figure 1(c) shows the schematic setup of the experiment. The generated photon pairs were first separated from the pump beam by mirror M_3 , which was coated with high reflectivity for 532 nm and high transmissivity for 1064 nm. A cutoff glass filter F was then used to suppress the pump photon further. The photon pairs were separated by a 50/50 beam splitter and then were, respec-

tively, collected into two single-photon detectors (Perkin Elmer SPCM-AQR-14), which were preceded by a pinhole (PH₁/PH₂) with 1 mm diameter, a collection lens (L_1/L_2) with $f = 50$ mm, and a 20 nm bandwidth interference filter (IF) centered at 1064 nm as shown in Fig. 1(c). The components above can be regarded as an assembly detector D_1 (D_2), whose detection position is defined by the position of pinhole PH₁ (PH₂). The distance z from the output surface of MPPLT to each detection plane was 1.4 m. The output electric pulses from D_1 and D_2 were then sent to a time correlation circuit with a coincidence window of 2.4 ns.

The two-photon far-field diffraction-interference pattern was measured by two schemes. In the first one, detector D_2 was fixed and D_1 scanned in the horizontal direction by the step size of 1 mm. Figure 2(a) shows the D_1 single counts and $D_1 - D_2$ coincidence counts versus the position of detector D_1 . In this figure, the D_1 single counts have an even distribution in a wide range, whereas the $D_1 - D_2$ coincidence counts exhibits the interference pattern in the range. The peak interval is about 7.41 mm, and the visibility of the fringe is 0.82 ± 0.03 . The resultant two-photon diffraction-interference pattern strongly resembles the first-order diffraction-interference pattern of a multislit grating (with the identical Λ_{tr} and b as the tested sample) by 1064 nm light. For comparison, moreover, we performed the same single and coincidence counting measurement on a periodically poled LiTaO₃ crystal without

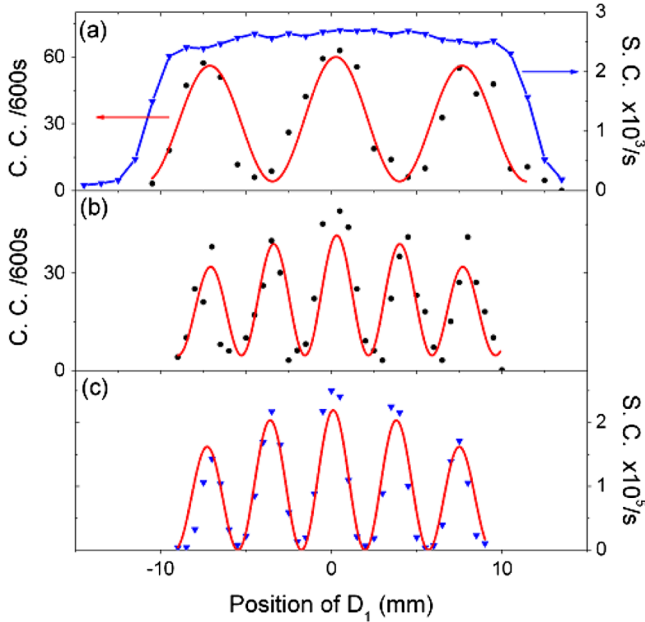


FIG. 2 (color online). (a),(b) Measurement of single and coincidence counts versus the position of detector D_1 . (a) D_2 was fixed. (b) D_1 and D_2 scanned in step. (c) Measurement of diffraction-interference pattern for the sample mask illuminated by the classical 532 nm light in the same experimental setup. The solid red curves in (a), (b), and (c) are theoretical fittings.

transverse modulation as shown in the inset of Fig. 3. As a result, the interference pattern was erased, and the coincidence counts demonstrated a single peak as shown in Fig. 3. The Gaussian-like coincidence peak results from the Fourier transformation of the pump profile in this case.

In the second scheme, both detectors D_1 and D_2 scanned along the same x direction by the step size of 0.5 mm synchronously. As expected, the $D_1 - D_2$ coincidence counts presented a second-order interference pattern as shown in Fig. 2(b). The peak interval is about 3.72 mm, exactly half of that in Fig. 2(a). This is a so-called two-photon subwavelength interference effect [23]. The two-photon behaves as an effective single photon but with the wavelength of a half. In comparison, a classical interference experiment of a multislit grating was performed using a 532 nm laser source. The multislit grating had the identical transverse modulation with the measured MPPLT. The result is shown in Fig. 2(c). Although the wavelength of the two-photon case is 1064 nm, which is twice that of classical 532 nm light, the diffraction-interference patterns are almost identical for these two cases.

The above results consist well with Eq. (6). The two-photon pairs can be generated from any one of the illuminated stripes in the MPPLT. This is similar in that two-photon pairs pass through a multislit grating and are diffracted by these slits at the same time. When one detector was fixed and the other moved, the optical path difference of the two-photon pairs from different strips depended only on the position of the moving detector. While the two detectors scanned in step, the optical path difference increased twice, so the peak interval of the interference pattern in the later situation should be reduced twice. In previous studies, the two-photon interference was observed by manipulating the pump beam profile [10,24], using two SPDC crystals [2] or placing a double slit at the output surface of the crystal [23]. In our experiment, the N -stripe grating was embedded intrinsically inside the nonlinear crystal and transformed the generated two-photon spatial

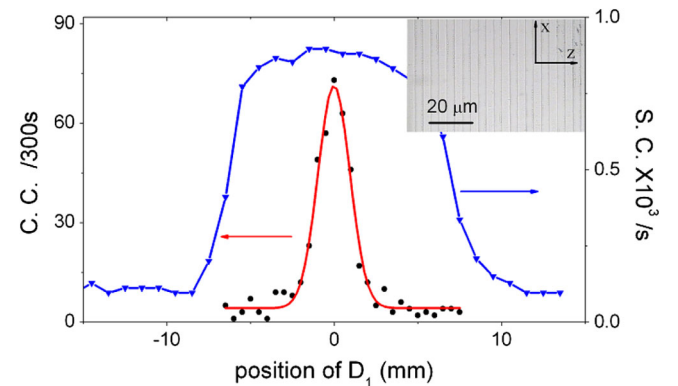


FIG. 3 (color online). Measurement of single and coincidence counts for the PPLT grating with no transverse modulation. Detector D_1 scanned, while D_2 was fixed. The inset shows the PPLT grating structure.

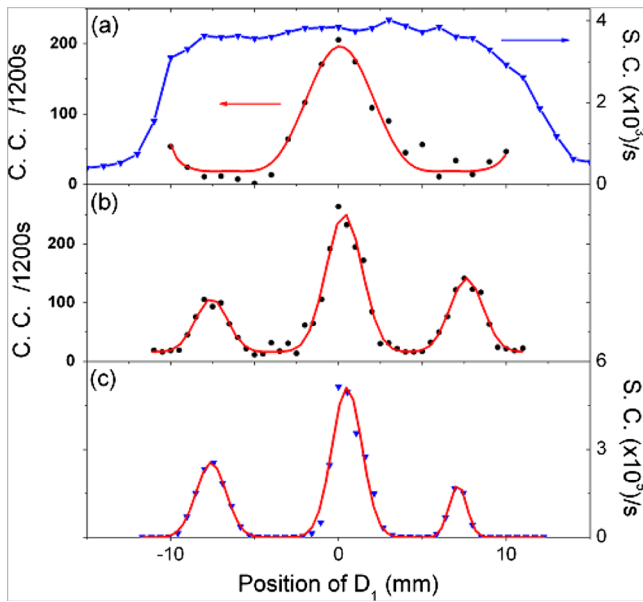


FIG. 4 (color online). (a),(b) Measurement of single and coincidence counts versus the position of detector D_1 for the MPPLT with $\Lambda_{tr} = 100 \mu\text{m}$, $b = 20 \mu\text{m}$, and $L = 4 \text{ mm}$. (a) D_2 was fixed. (b) D_1 and D_2 scanned in step. (c) Measurement of diffraction-interference pattern for the sample mask illuminated by the classical light 532 nm.

mode. Hence no accessional multislit grating or pump beam reforming was necessary. It suggests a new method to control and tailor the spatial entanglement of two-photon pairs by the technique of domain engineering.

To confirm the above conclusion, we took a similar measurement on another MPPLT with $\Lambda_{tr} = 100 \mu\text{m}$, $b = 20 \mu\text{m}$, and crystal length $L = 4 \text{ mm}$. The result is shown in Fig. 4. The peak interval of the diffraction-interference pattern is about 14.62 mm when only one detector scans. The interval is reduced twice when D_1 and D_2 scanned in step. The visibility of the coincidence fringe was 0.83 ± 0.02 . The experimental results also agree well with theoretical values according to Eq. (6).

In conclusion, we have experimentally studied the spatial mode of a two-photon entangled state produced from the transversely engineered QPM gratings. The spatial information of the MPPLT was transferred to the two-photon spatial mode, which was proved by the far-field diffraction-interference experiment. The QPM technique allows large variation of the spatial mode function over a small spatial scale in a single nonlinear crystal, so it is very favorable for integration and application. Moreover, by combining the longitudinal and transverse engineering of a QPM grating, we could construct the various space-momentum, time-energy, and spatial shape entanglement and even prepare the hyperentangled states [25]. The QPM

technique would be widely used in the design of quantum optics devices.

The authors thank Y. H. Shih for helpful discussions and technical assistance. This work is supported by the National Natural Science Foundation of China (No. 10534020) and by the National Key Projects for Basic Researches of China (No. 2006CB921804 and No. 2004CB619003).

*zhushn@nju.edu.cn; http://dsl.nju.edu.cn

- [1] M. H. Rubin, Phys. Rev. A **54**, 5349 (1996).
- [2] P. H. S. Ribeiro, M. F. Santos, P. Milman, and A. Z. Khoury, J. Opt. B **4**, S437 (2002).
- [3] A. Mair, A. Vaziri, G. Weihs, and A. Zeilinger, Nature (London) **412**, 313 (2001).
- [4] C. K. Law, I. A. Walmsley, and J. H. Eberly, Phys. Rev. Lett. **84**, 5304 (2000).
- [5] S. P. Walborn and C. H. Monken, Phys. Rev. A **76**, 062305 (2007).
- [6] D. Kaszlikowski, P. Gnaniński, M. Żukowski, W. Miklaszewski, and A. Zeilinger, Phys. Rev. Lett. **85**, 4418 (2000); D. Collins, N. Gisin, N. Linden, S. Massar, and S. Popescu, Phys. Rev. Lett. **88**, 040404 (2002).
- [7] N. J. Cerf, M. Bourennane, A. Karlsson, and N. Gisin, Phys. Rev. Lett. **88**, 127902 (2002).
- [8] G. Molina-Terriza, A. Vaziri, R. Ursin, and A. Zeilinger, Phys. Rev. Lett. **94**, 040501 (2005).
- [9] T. B. Pittman *et al.*, Phys. Rev. A **53**, 2804 (1996).
- [10] C. H. Monken, P. H. Souto Ribeiro, and S. Pádua, Phys. Rev. A **57**, 3123 (1998).
- [11] L. Neves *et al.*, Phys. Rev. Lett. **94**, 100501 (2005); A. Vaziri, G. Weihs, and A. Zeilinger, J. Opt. B **4**, S47 (2002).
- [12] J. P. Torres, A. Alexandrescu, S. Carrasco, and L. Torner, Opt. Lett. **29**, 376 (2004).
- [13] S. Tanzilli *et al.*, Electron. Lett. **37**, 26 (2001).
- [14] M. C. Booth *et al.*, Phys. Rev. A **66**, 023815 (2002).
- [15] S. Tanzilli *et al.*, Nature (London) **437**, 116 (2005).
- [16] S. E. Harris, Phys. Rev. Lett. **98**, 063602 (2007).
- [17] M. B. Nasr *et al.*, Phys. Rev. Lett. **100**, 183601 (2008).
- [18] S. Carrasco *et al.*, Opt. Lett. **29**, 2429 (2004).
- [19] A. V. Burlakov *et al.*, Phys. Rev. A **56**, 3214 (1997).
- [20] J. R. Kurz, A. M. Schober, D. S. Hum, A. J. Saltzman, and M. M. Fejer, IEEE J. Sel. Top. Quantum Electron. **8**, 660 (2002).
- [21] Y. Q. Qin, C. Zhang, Y. Y. Zhu, X. P. Hu, and G. Zhao, Phys. Rev. Lett. **100**, 063902 (2008).
- [22] G. Molina-Terriza, J. P. Torres, and L. Torner, Phys. Rev. Lett. **88**, 013601 (2001); S. Gröblacher, T. Jennewein, A. Vaziri, G. Weihs, and A. Zeilinger, New J. Phys. **8**, 75 (2006).
- [23] M. D'Angelo, M. V. Chekhova, and Y. H. Shih, Phys. Rev. Lett. **87**, 013602 (2001).
- [24] E. J. S. Fonseca, C. H. Monken, and S. Pádua, Phys. Rev. Lett. **82**, 2868 (1999).
- [25] J. T. Barreiro, N. K. Langford, N. A. Peters, and P. G. Kwiat, Phys. Rev. Lett. **95**, 260501 (2005).